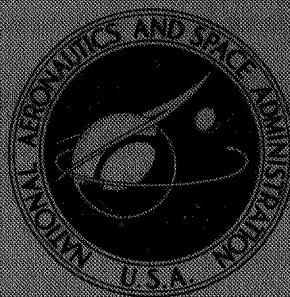


NASA TECHNICAL  
MEMORANDUM



NASA TM X-1503

NASA TM X-1503

FACILITY FORM 602

68-18893	
(ACCESSION NUMBER)	(THRU)
18	(CODE)
(PAGES)	(CATEGORY)
(NASA CR OR TMX OR AD NUMBER)	

DESIGN AND PERFORMANCE OF  
TWO VACUUM CHAMBERS AND  
SOLAR SIMULATORS FOR  
SOLAR-CELL RESEARCH

*by Adolph C. Spagnuolo*  
*Lewis Research Center*  
*Cleveland, Ohio*

NASA TM X-1503

DESIGN AND PERFORMANCE OF TWO VACUUM CHAMBERS AND SOLAR  
SIMULATORS FOR SOLAR-CELL RESEARCH

By Adolph C. Spagnuolo

Lewis Research Center  
Cleveland, Ohio

NATIONAL AERONAUTICS AND SPACE ADMINISTRATION

---

For sale by the Clearinghouse for Federal Scientific and Technical Information  
Springfield, Virginia 22151 - CFSTI price \$3.00

# DESIGN AND PERFORMANCE OF TWO VACUUM CHAMBERS AND SOLAR SIMULATORS FOR SOLAR-CELL RESEARCH

by Adolph C. Spagnuolo

Lewis Research Center

## SUMMARY

A facility containing a 5-foot- (1.52-m-) and a 2-foot- (0.61-m-) diameter space-environmental chamber with two solar-radiation simulators and support equipment is described. The facility is designed for testing solar cells, thermoelectric and thermionic devices, and related components at vacuum levels in the  $10^{-8}$  - to  $10^{-9}$ -torr ( $10^{-6}$  - to  $10^{-7}$ -N/m<sup>2</sup>) range. The pumping systems and liquid-nitrogen-cooled shrouds are described. Information concerning a test apparatus and a solar-cell installation method is also included.

## INTRODUCTION

New direct energy conversion devices, such as thin-film solar cells and flat-plate thermoelectric convertors, are being considered as sources of power for future space

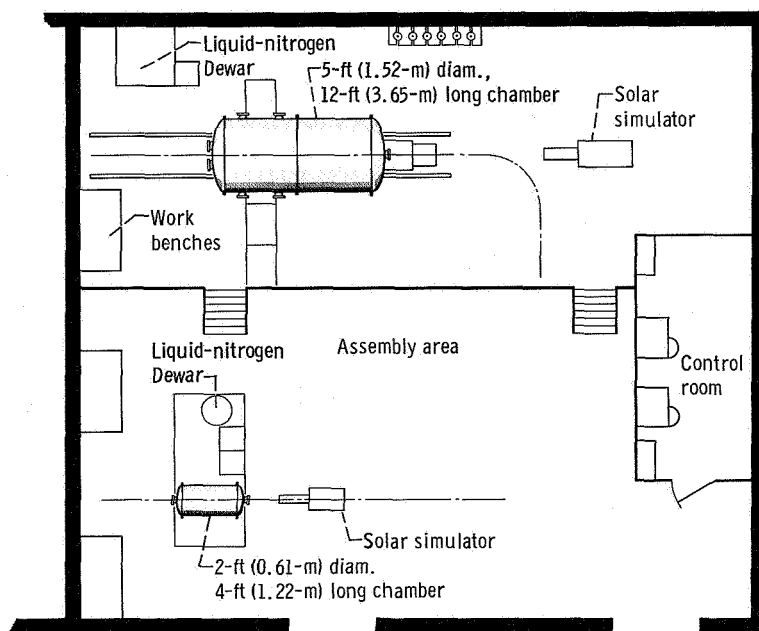
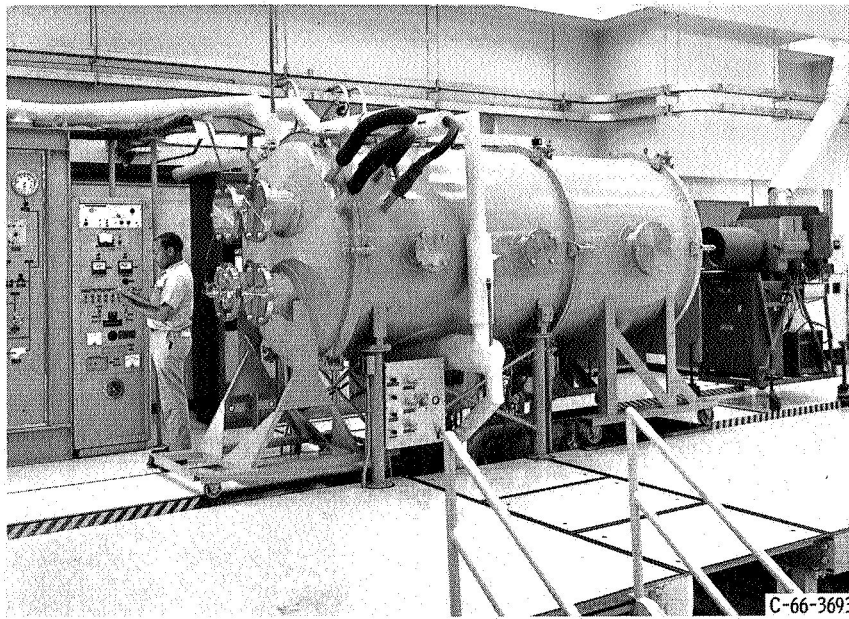
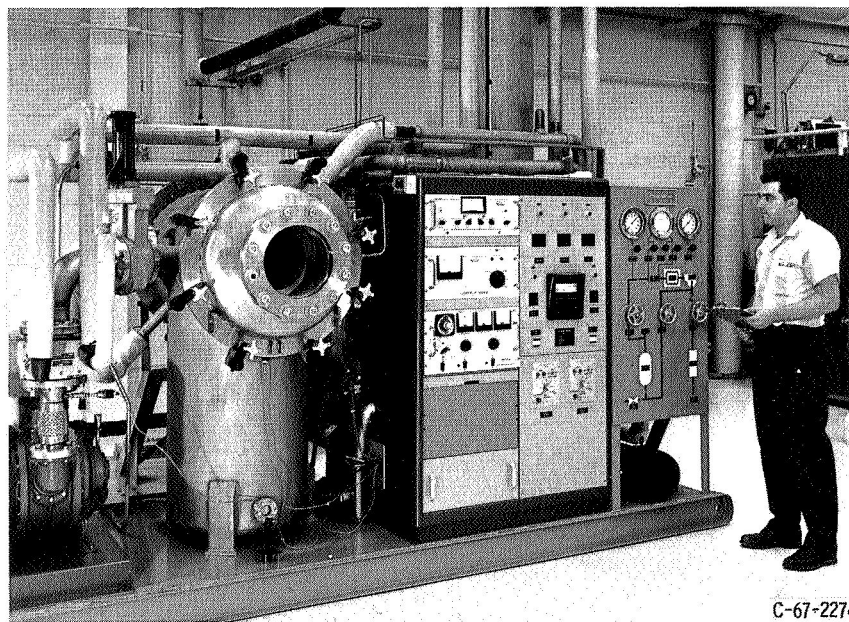


Figure 1. - Space-environmental laboratory.



C-66-3693

(a) Five-foot-(1.52-m-) diameter chamber.



C-67-2274

(b) Two-foot-(0.91-m-) diameter chamber.

Figure 2. - Space-environmental chambers.

exploration, and these devices require testing under simulated space conditions. The purpose of this report is to describe such a space-simulating facility.

The facility consists of a control room and an attached work area and houses two high-vacuum space-environmental chambers and two solar-radiation simulators with all necessary auxiliary equipment. A layout of the room is shown in figure 1. The 5-foot- (1.52-m-) diameter by 12-foot- (3.65-m-) long chamber (fig. 2(a)) is intended primarily for testing large segments of complete arrays at one solar constant (ref. 1)( $1400 \text{ W/m}^2$ ). The 2-foot- (0.61-m-) diameter by 4-foot- (1.22-m-) long chamber (fig. 2(b)), intended for testing the critical parameters of solar cell construction, is designed for fast pump-down and fast return to ambient conditions. Each space-environmental chamber is capable of operating at vacuum levels in the  $10^{-8}$ - to  $10^{-9}$ -torr ( $10^{-6}$ - to  $10^{-7}$ - $\text{N/m}^2$ ) range with its liquid-nitrogen shroud at  $77^{\circ} \text{ K}$ . The solar simulators, complementary to the chambers, will simulate the intensity of the sun from 0.30 to 16.0 solar constants. Data are presented that show pumpdown rates and the effect on chamber pressure of solar heating. Tests may be conducted in both chambers simultaneously with either solar radiation simulator.

### FIVE-FOOT- (1.52-m) DIAMETER CHAMBER

The 5-foot- (1.52-m) diameter test chamber is designed primarily for testing large segments of a solar cell array under space conditions at one solar constant. The chamber is 6 feet (1.82 m) long and is constructed from 1/4-inch- (6.35-mm-) thick 304-stainless-steel material. A 5-foot- (1.52-m-) diameter, 6-foot- (1.82-m-) long optical chamber mates to one end of the test chamber. The opposite end cover is roller-mounted and easily removable. Eight instrumentation ports are available around the chamber, two 10-inch (25.40-cm) ports on each of the two sides of the chamber, and four 12-inch (30.48-cm) ports located in the removable end cover. The arrangement of components, the major dimensions, the details of the vacuum feedthroughs, and other related information of the 5-foot- (1.52-m-) diameter chamber are shown in figure 3.

A 36-inch- (0.91-m-) diameter, 1-inch- (2.54-cm-) thick quartz window between the test chamber and the optical chamber allows testing of large arrays in the ultra-high-vacuum region because the window restricts the volume involved in the actual test compartment. A vacuum of about  $5.0 \times 10^{-6}$  torr ( $6.65 \times 10^{-4} \text{ N/m}^2$ ) is maintained in the optical chamber at all times during operation. The low-pressure differential across the quartz window allows the window to be of minimum thickness. The vacuum piping between the two chambers is free of any valves that could isolate one chamber from the other and result in a high-pressure load across the quartz window. These components

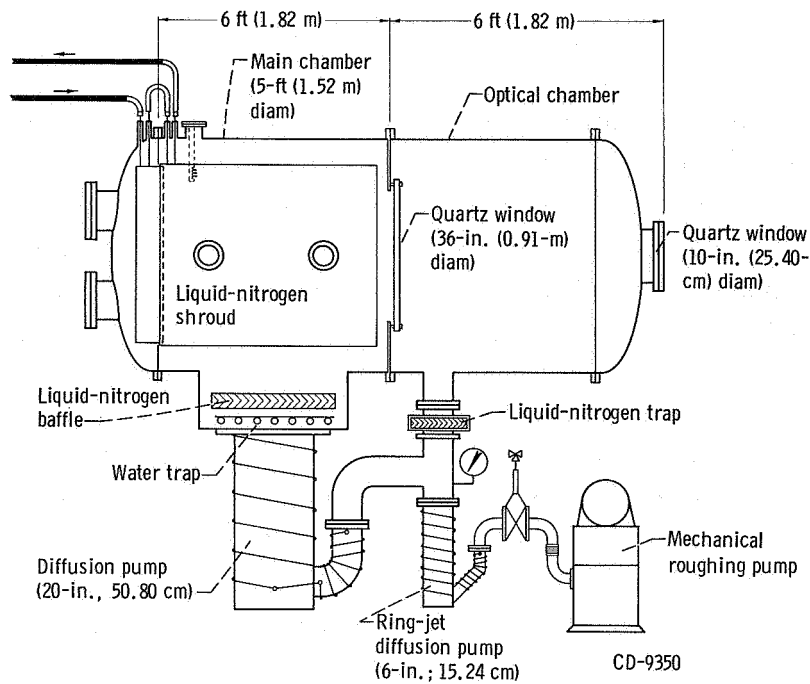


Figure 3. - Cutaway view of 5-foot-(1.52-m-) diameter chamber.

are shown in the cutaway view of the chambers (fig. 3). A 10-inch- (25.40-cm-) diameter quartz window is located in the optical chamber and provides an opening for the light from the solar simulator.

A liquid-nitrogen-cooled optically dense shroud surrounds the solar cell array and provides a thermal-radiation heat sink to simulate outer space. The shroud absorbs the solar radiation missing or scattered by the solar array, while the shroud's black coating keeps re-reflection to the solar array at a minimum. The shroud is constructed in two portions. The main portion is anchored to the 5-foot- (1.52-m-) diameter test chamber. The second portion is anchored to the removable end cover. Both portions are constructed from 1/8-inch- (3.17-mm-) thick 1100-0 aluminum with "D"-shaped tubing welded to the outside surface for liquid-nitrogen flow. The shroud is supported on rails and can be removed easily.

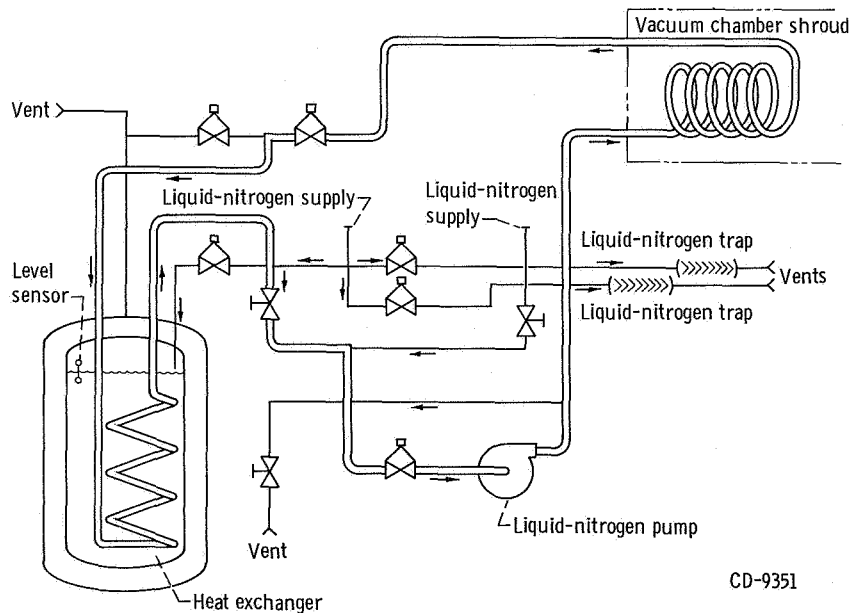
## PUMPING SYSTEM

The chamber is equipped with a vacuum pumping system to simulate deep-space conditions with normal testing in the  $10^{-8}$ - to  $10^{-9}$ -torr ( $10^{-6}$ - to  $10^{-7}$ -N/m<sup>2</sup>) range. The pumping system is shown in figure 3. Evacuation of the test chamber is accomplished by a combination of mechanical and diffusion pumps and cryopumping with liquid nitrogen. A mechanical pump (80 cu ft/min or 37.7 liters/sec) is used to rough down both the test

and optical chambers to  $1.5 \times 10^{-1}$  torr ( $19.95 \text{ N/m}^2$ ). Both diffusion pumps are then activated and become effective within 20 minutes. The 6-inch (15.24-cm) ring-jet diffusion pump is used to back up the 20-inch (50.80-cm) main diffusion pump and also to pumpdown the optical chamber. The 20-inch (50.80-cm) diffusion pump evacuates the main chamber down to the low  $10^{-6}$ -torr ( $10^{-4} \text{ N/m}^2$ ) range. The liquid-nitrogen-cooled shroud in the main chamber provides cryopumping in that section. There are 93 square feet ( $8.63 \text{ m}^2$ ) of aluminum surface designed to operate at  $77^\circ \text{ K}$ .

Backstreaming of oil from the diffusion pumps into the chambers is reduced to negligible amounts by liquid-nitrogen-cooled chevron-shaped traps over the inlets to both pumps. In addition, a water-cooled baffle is placed between the 20-inch (50.80-cm) diffusion pump and its liquid-nitrogen-cooled trap to further reduce oil backstreaming into the test chamber.

The liquid nitrogen supplied to the shroud is conserved by means of a liquid-nitrogen-to-liquid-nitrogen heat exchanger in a closed-loop system. In this system, warmed liquid nitrogen returns from the shroud and passes through a vacuum-jacketed Dewar, itself containing liquid nitrogen, where it is cooled and pumped back under pressure to the shroud (fig. 4). The liquid nitrogen from the Dewar boiloff is vented to the atmosphere, and the Dewar is replenished at all times from a second supply line. Liquid-nitrogen fill is maintained at predetermined levels by liquid level indicators located in the Dewar and in the traps above the diffusion pumps.



CD-9351

Figure 4. - Liquid-nitrogen flow diagram for 5-foot-(1.52-m-) diameter chamber.

## Chamber Controls and Facility Instrumentation

The vacuum level in both chambers and the foreline pressure are continuously monitored. Thermocouple vacuum gages are used to measure from atmospheric pressure to 1 micron, and ionization gages are used to measure pressure from 1 micron ( $10^{-1}$  N/m<sup>2</sup>) to  $1 \times 10^{-9}$  torr ( $1.33 \times 10^{-7}$  N/m<sup>2</sup>).

Vacuum thermocouple gages are located in the foreline, immediately before the roughing pump, and in the optical chamber. These gages are used to check mechanical pump performance during system pumpdown; to monitor diffusion pump prepressure during the vacuum cycle; and to indicate pressure reduction to the safe operating range of the ionization gage, thus preventing inadvertent filament burnout. The thermocouple gage readout is a two-station model mounted in a panel. The gage reads continuously down to 1 micron.

A thermocouple vacuum controller (vacuum gage) is located in the test chamber. In this pressure measuring device, a relay circuit serves as the controller. A pointer is adjusted to the desired control point on the direct-reading dial. As pressure decreases to the set point, a relay is energized and the diffusion pumps, liquid nitrogen (LN<sub>2</sub>) level controllers to the traps above the diffusion pumps, and LN<sub>2</sub> pump circuits are activated during automatic operation. The relay remains energized until the pressure rises above the set point. The gage reads continuously down to 1 micron.

A cold-cathode discharge gage is used to monitor pressure in the optical chamber continuously. The discharge tube is a Philips-gage and has a color-coded three-scale readout: 0.1 to 25 microns ( $1.33 \times 10^{-2}$  to  $3.325$  N/m<sup>2</sup>),  $1 \times 10^{-5}$  to  $1 \times 10^{-4}$  torr ( $1.33 \times 10^{-3}$  to  $1.33 \times 10^{-2}$  N/m<sup>2</sup>), and  $1 \times 10^{-7}$  to  $1 \times 10^{-5}$  torr ( $1.33 \times 10^{-5}$  to  $1.33 \times 10^{-3}$  N/m<sup>2</sup>).

A Bayard-Alpert nude ionization gage is used to monitor pressure in the test chamber continuously. The gage utilizes a nonburnout thoria-bonded filament with a 0.005-inch (0.102-mm) tungsten collector. The scales are in decades from  $1 \times 10^{-3}$  to  $1 \times 10^{-9}$  torr ( $10^{-1}$  to  $10^{-7}$  N/m<sup>2</sup>) with manual switching provided between ranges. Resistance degassing is accomplished simultaneously with normal operation of the gage.

Feedthroughs for 24 thermocouples are attached to one end cover port. These thermocouples are to monitor main-shroud and end-cover-shroud temperatures. Numerous feedthroughs are provided at the other ports for future use.

## Chamber Pressure

The performance characteristics of the vacuum system were determined for a clean, dry, empty chamber. The vacuum pumps may be operated in either the automatic or the manual mode. Since the performance level and the sequence of operation are the same for each mode, only the automatic mode will be described.

Positioning the selector switch to automatic mode starts the mechanical roughing pump and activates a time-delay relay set for 4.5 minutes. After the preset delay, the foreline valve opens and allows the entire system to be roughed down. When the pressure in the test chamber reaches  $1.5 \times 10^{-1}$  torr ( $19.95 \text{ N/m}^2$ ) the contacts on the thermocouple vacuum controller (vacuum gage) will close and activate the circuits to the diffusion pumps, the liquid-nitrogen level controllers to the traps above the diffusion pumps, and the  $\text{LN}_2$  pump. While the diffusion pumps are evacuating the test chamber, cold gas is circulating in the shroud. The  $\text{LN}_2$  pump is primed and manually started when the vacuum in the test chamber reaches the  $10^{-4}$ -torr ( $10^{-2} \text{ N/m}^2$ ) range. The system is then completely operational and will maintain this condition until manually stopped.

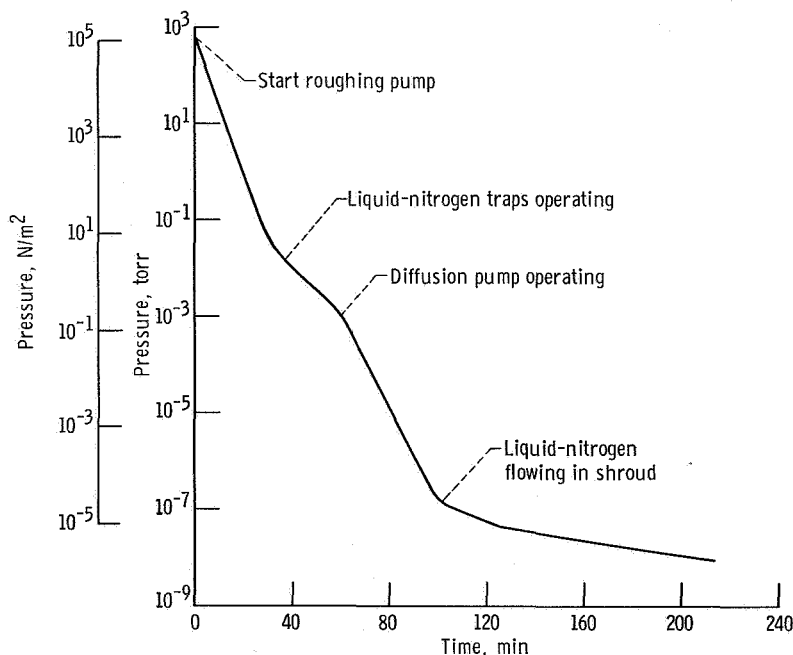


Figure 5. - Five-foot- (1.5-m-) diameter chamber pumpdown rate with liquid-nitrogen-cooled traps and shroud and water-cooled baffle above 20-inch (50-cm) diffusion pump.

The performance of the clean, empty chamber is shown in figure 5. From the curve, it can be seen that the system is capable of evacuation to  $1 \times 10^{-8}$  torr ( $1.33 \times 10^{-6} \text{ N/m}^2$ ) in 3.5 hours. Further, the ultimate pressure has not been reached, since the slope of the pressure-time curve has a value less than zero. The pumping regimes are identified in the figure.

An additional test was performed to determine the influence of the solar simulator on the vacuum level and thermal properties of the chamber. A 30- by 30-inch (76.20- by 76.20-cm) square plate was coated with a black paint to simulate the absorptivity, emissivity (0.9), and temperature ( $60^\circ \text{ C}$  ( $333^\circ \text{ K}$ )) expected of solar-cell arrays to be tested in the chamber.

The solar simulator was placed at a distance of 20 feet (6.09 m) to produce 1 solar constant on the plate. At a base vacuum level of  $1.2 \times 10^{-8}$  torr ( $1.59 \times 10^{-6}$  N/m<sup>2</sup>), the simulator was turned on. The vacuum level in the main chamber went up to  $3.8 \times 10^{-8}$  torr ( $5.05 \times 10^{-6}$  N/m<sup>2</sup>) in approximately 17 minutes; however, with continuous pumping most of this pressure rise was recovered, and the ionization gage settled out at  $2.0 \times 10^{-8}$  torr ( $2.66 \times 10^{-6}$  N/m<sup>2</sup>). Within the next 40 minutes, the steady-state plate temperature was recorded as 70° C (343° K). The test was then repeated with the simulator at a distance of 14 feet (4.26 m) from the plate to produce a solar constant of two suns. At a base vacuum level of  $1.2 \times 10^{-8}$  torr ( $1.59 \times 10^{-6}$  N/m<sup>2</sup>), the simulator was turned on. The pressure went up to  $2.3 \times 10^{-8}$  torr ( $3.05$  N/m<sup>2</sup>) and settled out at a reading of  $2.0 \times 10^{-8}$  torr ( $2.66$  N/m<sup>2</sup>).

The equilibrium temperature (70° C or 343° K) of the plate at 1 solar constant is only slightly higher than the expected temperature rise (60° C or 333° K) of a solar-cell array. The main-shroud temperature was not affected by the radiation from either the solar simulator or the warm panel.

## Solar-Cell Installation

Solar-cell arrays are mounted on the test fixture and cantilevered from the chamber end cover. The complete assembly takes place outside the test chamber. The circular ring holding the array allows for positioning of the array in two planes prior to testing. All power and instrumentation feedthroughs are located in the end cover. After the solar

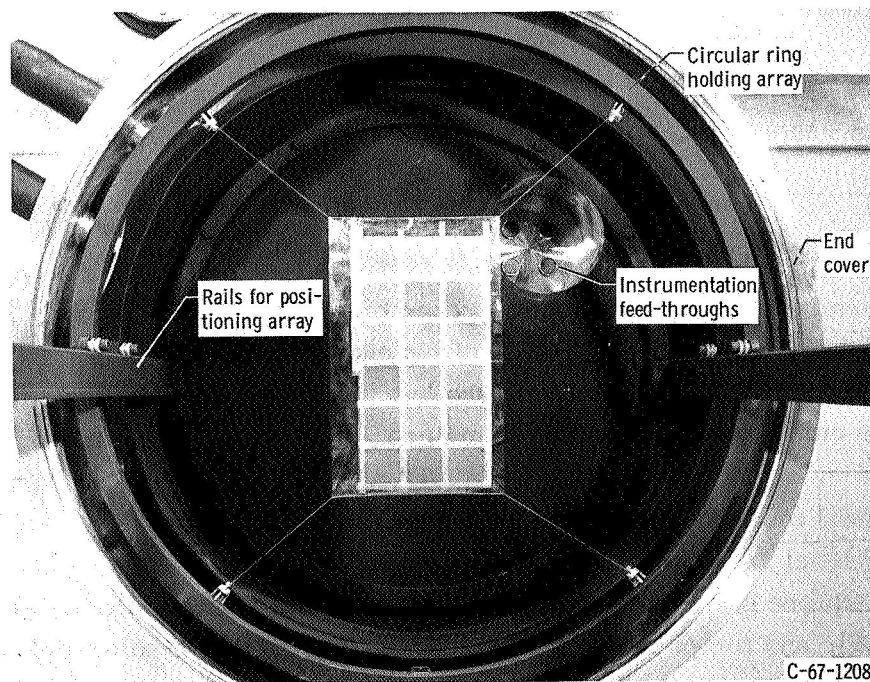


Figure 6. - Test fixture for mounting solar cell array.

array is assembled, the end cover is rolled into the operating position on a set of rails. A typical solar-cell array assembly is shown in figure 6.

### Two-Foot- (0.61-m-) Diameter Chamber

The 2-foot- (0.61-m-) diameter by 4-foot- (1.22-m-) long chamber is used mainly for testing the critical electrical and mechanical parameters of single solar-cell construction under space conditions at 1 or more solar constants. For this purpose, the system was designed for fast pumpdown and fast return to laboratory ambient conditions. The getter-ion pumping systems of the chamber, which are used to obtain the proper pumpdown rates, have the desirable features of providing (1) ultrahigh vacuum, (2) a clean system, free of organic vapor, and (3) continuous unattended operation.

Description. - The chamber walls are constructed of 1/4-inch- (6.35-mm-) thick 304-stainless-steel material. A 10 $\frac{1}{2}$ -inch- (26.67-cm-) diameter quartz window is located in one end cover to provide an opening for the light from the solar simulator. The opposite end cover is easily removable and contains the test fixture for mounting solar cells. Both end covers are roller mounted on an inverted steel angle. The arrangement of chamber components is shown in figure 7.

A liquid-nitrogen-cooled optically dense shroud lines the entire portion of the test chamber except for the 10 $\frac{1}{2}$ -inch- (26.67-cm-) diameter quartz window. The cryogenic

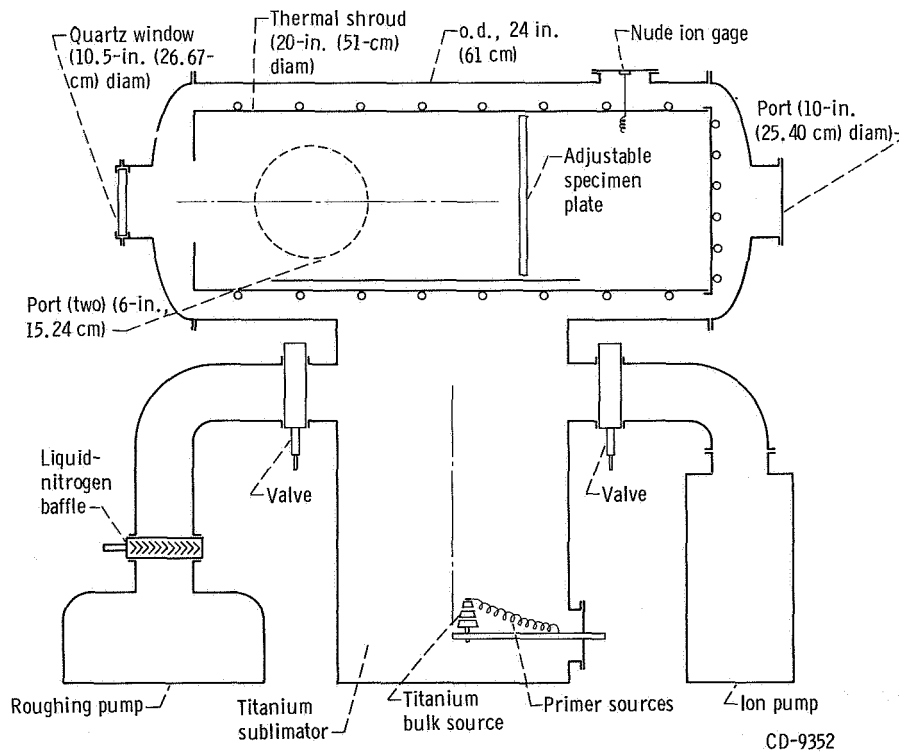


Figure 7. - Cutaway view of 2-foot-(0.61-m-) diameter chamber.

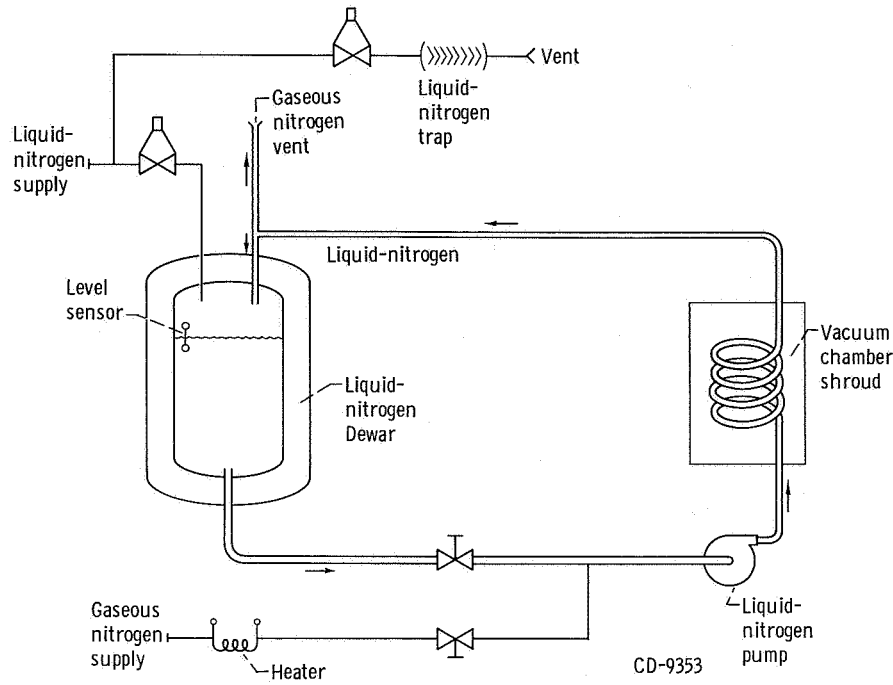


Figure 8. - Liquid-nitrogen flow diagram for 2-foot-(0.61-m-) diameter chamber.

system is shown in figure 8. This system is skid mounted and consists of a LN<sub>2</sub> pump, an intermediate storage tank, a thermal shroud, and a LN<sub>2</sub> baffle. Single-phase LN<sub>2</sub> flow is maintained throughout the shroud. The nitrogen from the shroud is returned to the storage tank, where a portion of the LN<sub>2</sub> is vaporized and vented to the atmosphere outside the room. Makeup nitrogen is then introduced to the tank from the supply line. Solenoid valves and LN<sub>2</sub> level indicators are used to supply and maintain the LN<sub>2</sub> cold trap and storage tank.

The thermal shroud is also designed to warm up from -320<sup>o</sup> F (77<sup>o</sup> K) to ambient temperature in 30 minutes. The warmup system utilizes the same flow passages as the LN<sub>2</sub>. A 5-kilowatt electric heater is used to heat the gaseous nitrogen (GN<sub>2</sub>) as it flows from an external supply into the shroud.

Pumping system. - The pumping system is shown in figure 7. A roughing pump evacuates the chamber to the low-micron range. At this time, liquid nitrogen flowing through the shroud, inside the chamber, provides cryopumping and lowers the chamber pressure to the middle 10<sup>-5</sup>-torr (10<sup>-3</sup>-N/m<sup>2</sup>) range. Titanium sublimation is used to handle the heavy gas loads in the 10<sup>-5</sup>-torr (10<sup>-3</sup>-N/m<sup>2</sup>) range, while an ion pump is used to pump the noble gases and continues to lower chamber pressure to the 10<sup>-8</sup> - to 10<sup>-9</sup>-torr (10<sup>-6</sup> - to 10<sup>-7</sup>-N/m<sup>2</sup>) range.

Two protection devices have been designed into the pumping system to prevent contaminations of the chamber and the ion pump and to assure that shutdown intervals for cleaning the system are kept to a minimum. Backstreaming of oil from the mechanical

pump is reduced to negligible amounts by a liquid-nitrogen-cooled chevron-shaped trap. A stainless-steel pneumatically operated gate valve is located at the entrance to the ion pump and may be closed in case of vacuum failure or during periods in which the chamber is open to the atmosphere. During these times, the ion pump need not be shut off and is thus ready for immediate restart of the pumping.

Chamber instrumentation. - Chamber vacuum levels are continuously monitored by a Pirani-type thermocouple gage and a nude ion gage. A two-station thermocouple gage is used to read pressures from atmospheric to 1 micron ( $1.33 \times 10^{-1} \text{ N/m}^2$ ); one tube is located in the mechanical pump roughing line and one tube in the chamber. The exposed sensing element of the ion gage is located inside the cold shroud through a penetration in the shroud. Ionization-gage pressure is indicated on a linear decade scale used in conjunction with an eight-position switch that permits the selection of full-scale pressures from  $10^{-4}$  to  $10^{-10}$  torr ( $10^{-2}$  to  $10^{-8} \text{ N/m}^2$ ).

## CHAMBER PERFORMANCE

The performance characteristics of the vacuum system are presented in figure 9. The four stages of the pumpdown are indicated by the curve. With the vacuum and cryogenic systems initially at ambient conditions, the chamber obtains a vacuum of  $1 \times 10^{-8}$  torr ( $1.33 \times 10^{-6} \text{ N/m}^2$ ) in 1 hour and 50 minutes. These data are obtained with the chamber clean, dry, and empty.

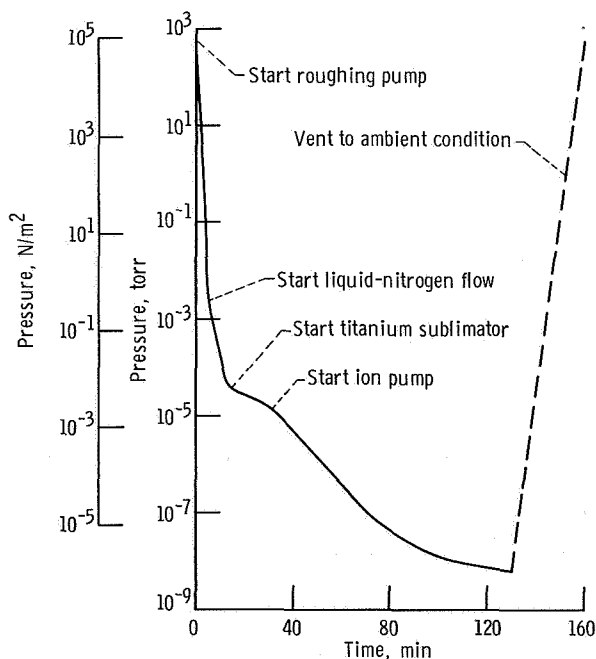


Figure 9. - Two-foot- (0.61-m-) diameter chamber pumpdown.

Approximately 30 minutes are required for the complete facility to return to ambient conditions. Nitrogen gas heated to 66<sup>o</sup> C (339<sup>o</sup> K) is utilized in bringing the liquid-nitrogen shroud back to ambient temperature. The chamber pressure is then returned to ambient by backfilling the chamber with dry nitrogen gas.

## SOLAR-RADIATION SIMULATORS

Two carbon-arc solar-radiation simulators (A and B) are in operation to support the vacuum chambers. Performance characteristics of the two simulators were determined and are presented in table I. Each simulator was tested at 1 solar constant in air.

Higher intensities can be obtained by moving the target closer to the source. However, the available target size is correspondingly reduced, and uniformity of irradiance may be sacrificed. With some modifications to the optical system of simulator B, a 4-inch by 4-inch (10.16-cm by 10.06-cm) area was irradiated with 16.3 solar constants with a uniformity of ±6 percent.

TABLE I. - PERFORMANCE CHARACTERISTICS OF  
CARBON ARC SOLAR RADIATION SIMULATORS

Condition	Simulator	
	A	B
Intensity, mW/cm <sup>2</sup>	140	140
Target plane diameter, in.	48	30
cm	121.92	76.20
Distance from last lens to target, ft	12	20
m	3.65	6.09
Beam divergence (full angle), deg	<sup>a</sup> 18.5	<sup>b</sup> 7.0
Stability, percent	<sup>c</sup> ±6.0	<sup>d</sup> ±1.30
Integrated radiant power output, W	1313	733
Efficiency, percent	4	6.8

<sup>a</sup>Obtained from dimensions of 50-in. (127.00-cm) beam at distance of 12 ft (3.65 m).

<sup>b</sup>Obtained from dimensions of 40-in. (101.60-cm) beam at distance of 20 ft (6.09 m).

<sup>c</sup>Twenty-minute period.

<sup>d</sup>Thirty-minute period.

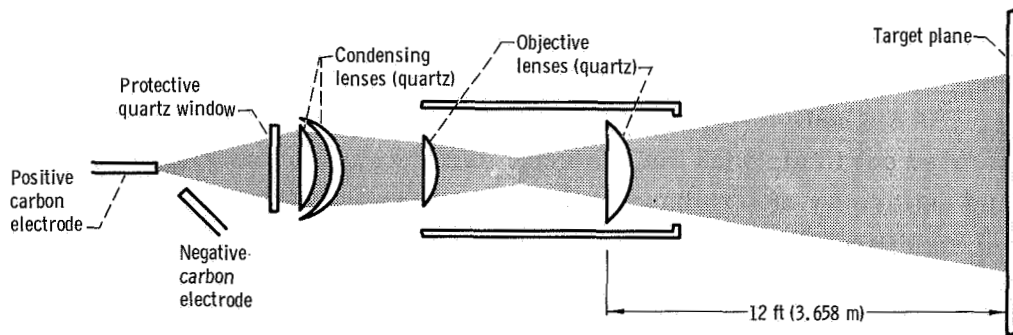
Testing can be conducted in both chambers simultaneously with either solar simulator.

## Simulator A

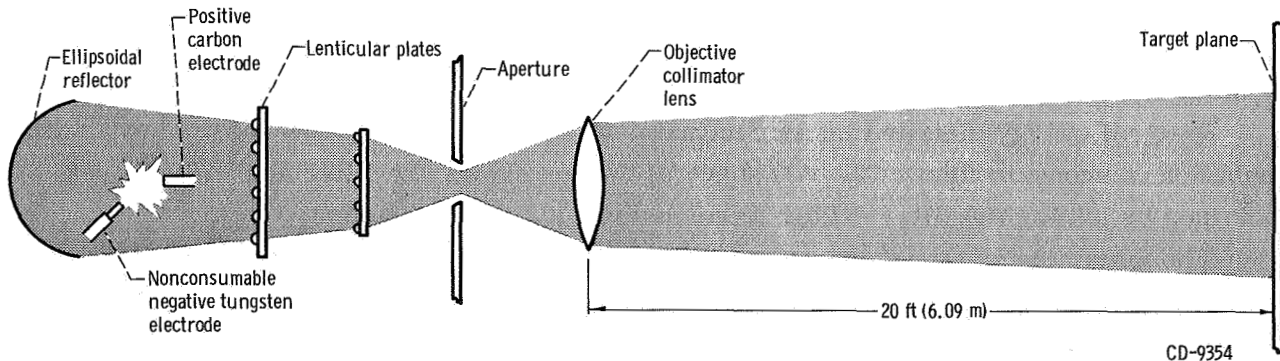
The three main components to simulator A (ref. 2) are (1) an arc lamp and housing (2) a nosepiece containing the optical system, and (3) a silicon-rectifier direct-current power supply.

The arc lamp employs a one-piece negative-electrode holder and a split-jaw positive-electrode holder. Both electrodes are mechanically advanced by a single drive motor. An electro-optical device automatically maintains the positive electrode at a constant protrusion. The optical system (fig. 10(a)) is composed of two fixed condensing lenses located in a water-cooled holder very close to the arc, and two movable planoconvex objective lenses located in the optical nosepiece.

The power supply is a silicon rectifier type with an input rating of 440 volts, 60 cycle, 3 phase, 85 amperes, and an adjustable output to 410 amperes at 72 to 85 volts direct-current full load, and 110 to 120 volts direct current no load.



(a) Simulator A.



(b) Simulator B.

Figure 10. - Optical systems for solar simulators.

## Simulator B

The three main components to simulator B (ref. 3) are (1) an arc lamp and housing (2) a nosepiece containing the aperture and objective lens or collimator, and (3) a selenium-rectifier direct-current power supply.

The arc lamp consists basically of a positive electrode assembly, a negative electrode assembly, and provisions for starting and maintaining the arc. The negative electrode is a nonconsumable argon-bathed tungsten rod that replaces the conventional carbon negative electrode. All cooling is integrated into the system, although the lamp housing must be vented to an external exhaust.

The optical system (fig. 10(b)) consists of an ellipsoidal aluminized reflector. The converging beam leaving the collector passes through a pair of molded lenticular plates, or mosaic lenses. The final optical element is a biconvex quartz projection lens serving as the collimator.

The power supply is a selenium-rectifier type with an input rating of 19 kilovolt-amperes, 230 volts, 60 cycles, 3 phase, and an adjustable output current of 200 amperes at 60 volts direct current full load, and 80 volts direct current no load.

## PERFORMANCE

An evaluation of the performance characteristics of simulators A and B (ref. 4) was carried out in air with the essential solar simulator parameters, such as (1) irradiance and uniformity of irradiance, (2) spectral energy distribution, (3) beam divergence, and (4) stability.

## Simulator A

Irradiance and uniformity of irradiance refer to the total intensity and the point-to-point intensity variation in the target plane. Scans were completed at a 12-foot (3.6-m) distance. Polar plots showing intensity distribution are given in figure 11. The overall system efficiency was 4.0 percent.

Spectral energy distribution as compared with the Johnson extraterrestrial solar distribution is shown in figure 12. All spectral curves shown are filter equivalents (ref. 5) obtained by joining the filter center wavelengths with straight lines.

The maximum full-angle divergence is  $18.5^{\circ}$  as obtained from the dimension of a 50-inch (1.27-m) beam at a distance of 12 feet (3.65 m) from the exit lens which has a  $3\frac{1}{4}$ -inch (8.25-cm) beam diameter at the exit lens.

Measurements on the long term stability of beam intensity were limited to about 20 minutes or about the stable period of one positive electrode. A  $\pm 6$ -percent variation was recorded during the consumption of any one electrode.

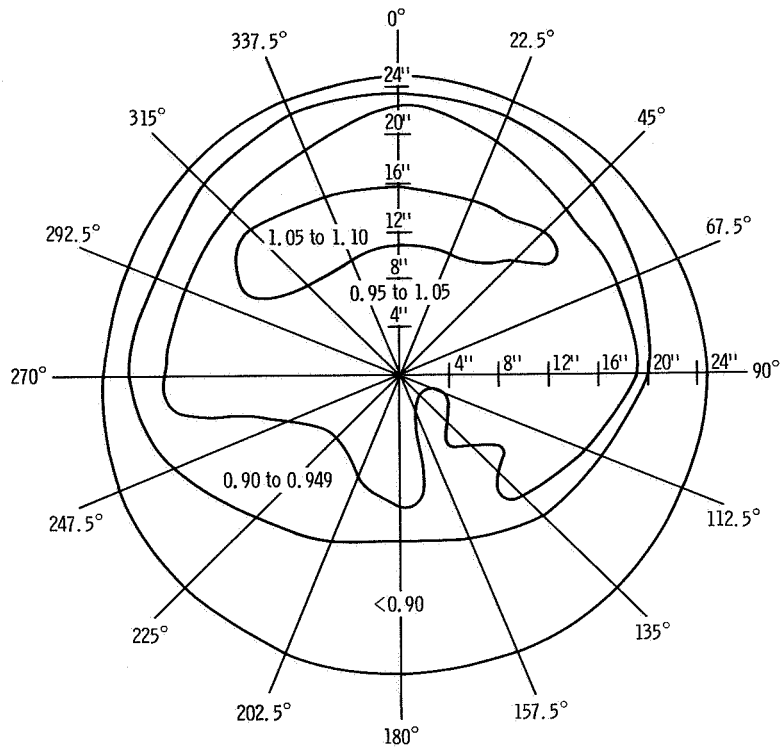


Figure 11. - Intensity distribution of simulator A at 12 feet (3.65 m). Values are in solar constants.

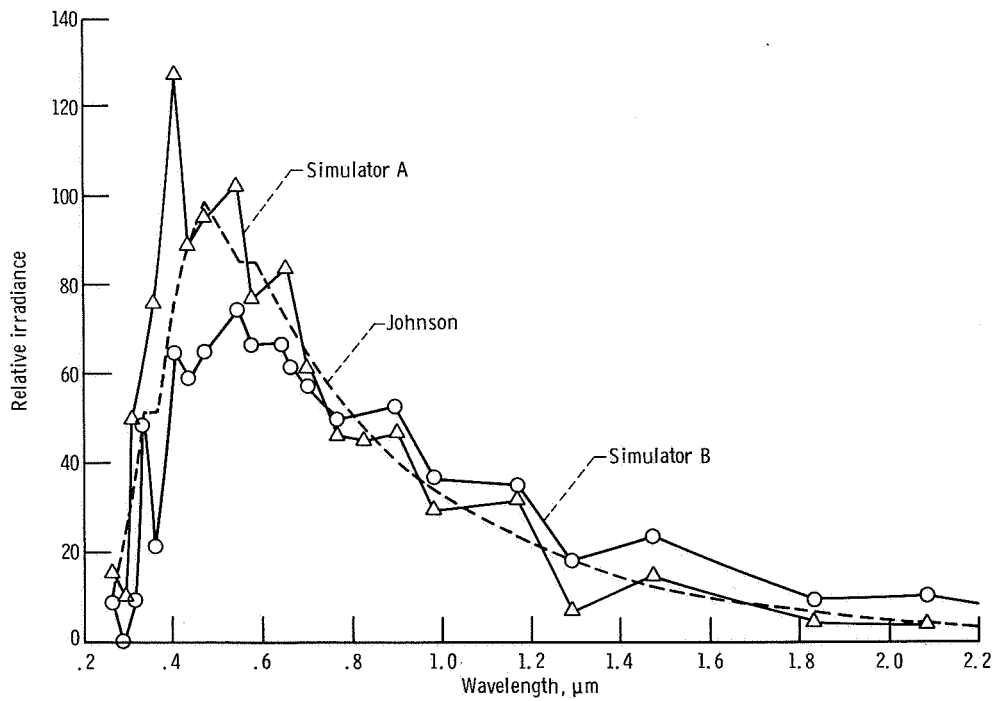


Figure 12. - Comparison of spectral energy distribution of simulators A and B with Johnson's extraterrestrial sun curve.

## Simulator B

A profile plot showing the intensity distribution at 1 solar constant across the  $90^\circ$  to  $270^\circ$  diameter is shown in figure 13. Scans were completed at 20-foot (6.09-m) target distances. Uniformity is readily apparent from the plot. The system efficiency was 6.8 percent.

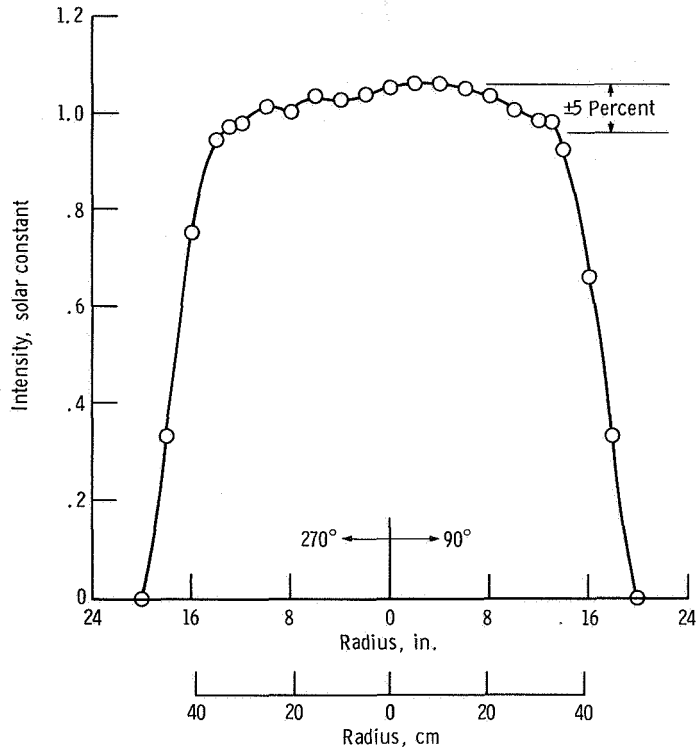


Figure 13. - Intensity distribution of simulator B with nonconsumable negative electrode at 20-foot (6.09-m) target distance.

Spectral energy distribution as compared with the Johnson extraterrestrial solar distribution is shown in figure 12. Here again, all spectral curves shown are filter equivalents (ref. 5).

The maximum full-angle divergence is  $7^\circ$  as obtained from the dimension of a 40-inch (101.60-cm) beam at a distance of 20 feet (6.09 m) from the exit lens, which has a 10-inch (25.40-cm) beam diameter at the exit lens.

The long-time stability of beam intensity was limited to about 30 minutes or about the stable period of one positive electrode. A 1.3-percent variation was recorded during the consumption of any one electrode.

## CONCLUDING REMARKS

The layout and performance of the solar-radiation space-environmental laboratory facilities at the NASA Lewis Research Center were described. These facilities consist primarily of two space-environmental chambers and two carbon-arc solar-radiation simulators. Tests may be conducted in a space environment with vacuum levels in the  $10^{-9}$  - to  $10^{-8}$  -torr ( $10^{-7}$  - to  $10^{-6}$  - $N/m^2$ ) range with liquid-nitrogen heat-sink temperatures in either chamber.

Pressures of  $1 \times 10^{-8}$  torr ( $1.33 \times 10^{-6}$   $N/m^2$ ) can be reached and maintained within 1 hour and 50 minutes in the 2-foot- (0.61-m-) diameter chamber, while a time of 3 hours and 30 minutes is required in the 5-foot- (1.52-m-) diameter chamber. The outgassing of a test specimen when it is irradiated with a solar simulator causes a small pressure rise in the chamber. However, with continuous pumping, most of the pressure rise is recovered within a short time.

Lewis Research Center,  
National Aeronautics and Space Administration,  
Cleveland, Ohio, September 12, 1967,  
120-33-01-10-22.

## REFERENCES

1. Johnson, Francis S.: The Solar Constant. J. Meteorol., vol. 11, no. 6, Dec. 1954, pp. 431-439.
2. Anon.: Solar Radiation Simulator Model ME 6, Form 333C, Genarco Inc.
3. Anon.: Arcomatic Solar Radiation Simulator, Form 231-B, Strong Electric Corp.
4. Goldman, Gary C.; and Yass, Kenneth: Performance of 10-Kilowatt-Carbon-Arc Solar Radiation Simulator. NASA TM X-1411, 1967.
5. Wagoner, Ralph E.; and Pollack, John L.: Data Reduction for Filter Spectroradiometry. NASA TN D-3037, 1965.